2011 American Control Conference
on O'Farrell Street, San Francisco, CA, USA
June 29 - July 01, 2011

Optimal H_∞ Control For Hard Disk Drives With An Irregular Sampling Rate

Jianbin Nie, Edgar Sheh, and Roberto Horowitz

***Abstract*— This paper discusses the optimal H_∞ control synthesis via discrete Riccati equations for hard disk drives (HDDs) with an irregular sampling rate. A HDD servo system with an irregular sampling rate, caused by missing position error signal sampling data, is modeled as a linear periodically time-varying (LPTV) system. An optimal H_∞ track-following control algorithm for HDD servo systems with irregular sampling rates is proposed, which is based on the previous H_∞ synthesis results for LPTV systems developed by some of the authors. A simulation and implementation study demonstrates that the proposed control synthesis technique is able to handle the irregular sampling rate and can be used to conveniently design a loop-shaping track-following servo that achieves the robust performance of a desired error rejection function for disturbance attenuation. Implementation results on an actual hard disk drive validate the simulation results.**

I. INTRODUCTION

Since a hard disk drive (HDD) servo system with regular sampling rates can be modeled as a linear time-invariant (LTI) system [3] and the control theory for LTI systems is well developed, maintaining a regular sampling rate is quite attractive for HDD servos. However, the sampling interval for HDD servo systems is not always equidistant and even sometime an irregular sampling rate due to missing position error signal (PES) data is unavoidable. For example, false PES demodulation, due to incorrect servo address mark (SAM) detection [6] or damaged servo patterns in several servo sectors, makes the feedback PES unavailable in those servo sectors, resulting in an irregular sampling rate. In this paper, the unavailability of feedback signals at a given sampling instance is referred as a "missing sample". In addition, irregular sampling rates also frequently occur during the self-servo track writing (SSTW) process [2]. For example, during some SSTW processes, the time of writing final concentric servo patterns may coincide with the time of reading the feedback position error signal from previously written servo patterns. This conflict, caused by the fact that an HDD servo system can not read and write at the same time, is referred as a "collision" of reading the PES with writing the final servo pattern. Such a collision makes the feedback signal unavailable resulting in an irregular sampling rate. Thus, it is important to address the issue of designing servo systems for HDDs under irregular sampling rates. Generally speaking, the location of damaged servo sectors and the collision in the self-servo track writing process is consistent on each single servo track. Therefore, the unavailability of PES for HDD servo systems takes place in some fixed and pre-determined positions for a given track. Furthermore, by considering that the natural periodicity of HDDs is related to the disk rotation, these servo systems can be represented as linear periodically time-varying systems with period equal to the number of servo sectors.

Furthermore, since there tend to be large variations in HDD dynamics due to the variations in manufacturing and assembly, it is not enough to achieve adequate servo performance for a single plant. Therefore, the designed controllers must guarantee a pre-specified level of performance for a large set of HDDs. By utilizing classical loop-shaping ideas which are familiar to most practicing engineers, the H_∞ loop-shaping control design [13] is well-suited to deal with the robust performance of the desired loop shape. Using such control, a set of HDDs with plant variations and a regular sampling rate is able to yield a desired error rejection function for disturbance attenuation [7]. Thus, optimal H_∞ control is quite attractive for HDD servo systems. The purpose of this paper is to extend these results to HDDs with missing PES samples.

In this paper, we consider the optimal H_∞ control design for HDD servo systems with irregular sampling rates. First, these systems are modeled as linear periodically time-varying systems, by considering the natural periodicity of hard disk drives, which is related to the disk rotation. Then, an optimal H_∞ controller can be synthesized using the control design methodologies for LPTV systems presented in [9]. The H_∞ control synthesis methodology presented in [9] requires the solution of a set of discrete Riccati equations. As discussed in [5], the synthesis methodologies based on the solution of discrete Riccati equations are often significantly more computationally efficient and numerically robust than comparable methodologies based on the solution of semi-definite programs (SDP) involving optimization problems constrained by linear matrix inequalities (LMIs). Moreover, with the developed control synthesis technique, the HDD servo systems with irregular sampling rates can still achieve the robust performance of an adequate error rejection function for disturbance suppressions.

In order to demonstrate the effectiveness of the developed control algorithm, we apply it to the track-following control of a real hard disk drive with missing PES samples. However, because the total number of PES samples in a HDD revolution is large and the resulting controller is periodically time-varying, a significant amount of memory is required to store all of the control parameters. Thus, in order to reduce the

J. Nie and R. Horowitz are with Department of Mechanical Engineering, University of California, Berkeley (email: njbin@berkeley.edu and horowitz@berkeley.edu)
E. Sheh is with Western Digital Corporation. (email: edgar.sheh@wdc.com)

memory storage requirements, a simplified controller implementation is developed in this paper, which utilized a reduced number of periodic control parameters. The simulation study presented in this paper validates the effectiveness of the proposed control synthesis algorithm and the feasibility of the control simplification, while the implementation results verify the simulation results and furthermore illustrate that the proposed control is implementable in real HDDs.

This paper is organized as follows. Section II discusses the modeling of HDD servo systems with an irregular sampling rate. In Section III, the optimal H_∞ control algorithm is provided. The application for the developed control algorithm is presented in Section IV. Conclusions are given in Section V.

II. Modeling of HDD Servo Systems with An Irregular Sampling Rate

As discussed in the previous section, an irregular sampling rate can be caused by missing a sample when the feedback PES is unavailable. Similarly to [1], HDD servo systems with irregular sampling rates can be modeled by the block diagram shown in Fig. 1. Here, we consider the output multiplicative uncertainty with the nominal plant of the voice coil motor (VCM) G_v^n and the plant uncertainty weighting function $W_\triangle$ as

$$G_v = \left(1 + W_\triangle \triangle\right) G_v^n, \quad \|\triangle\|_\infty \le 1 \,. \tag{1}$$

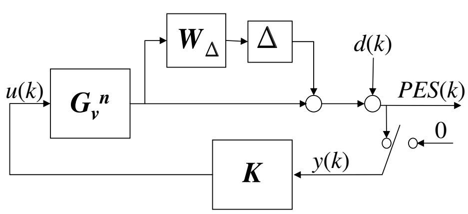

Fig. 1. Modeling of HDD servo systems with an irregular sampling rate

In Fig. 1, d is the overall contribution of all disturbances [10] including torque disturbance, windage, non-repeatable disk motions and measurement noise to PES. In addition, K is the controller to be designed by using the feedback signal $y(k)$ even a PES sample is missing. Notice that y is switched to PES when the PES sample is available, while y is switched to zero when the PES sample is unavailable [8]. Then, the servo system with the irregular sampling rate has the following state-space realization:

$$G_o \sim \begin{bmatrix} x(k+1) \\ y(k) \end{bmatrix} = \left[\begin{array}{c|cc} A^o & B_1^o & B_2^o \\ \hline C_2^o(k) & D_{21}^o(k) & 0 \end{array}\right] \begin{bmatrix} x(k) \\ d(k) \\ u(k) \end{bmatrix} \,. \tag{2}$$

Here, all of matrices except $C_2^o(k)$ and $D_{21}^o(k)$ in the above state-space realization are constant and

$$\begin{bmatrix} C_2^o(k) & D_{21}^o(k) \end{bmatrix} = \begin{cases} \begin{bmatrix} C_{2m}^o & D_{21m}^o \end{bmatrix} & \text{if } PES(k) \text{ is available} \\ \begin{bmatrix} 0 & 0 \end{bmatrix} & \text{otherwise} \end{cases} \,.$$

Since the location of damaged servo sectors and the collision in the self-servo track writing process is fixed for each servo track, the unavailability of the PES for HDD servo systems takes place at some fixed and pre-determined locations [2] on the disk for each track. Furthermore, by considering that the natural periodicity of HDDs is related to the disk rotation, the servo systems can be represented as LPTV systems with the state-space realization in (2) whose elements are periodic, for example, $\begin{bmatrix} C_2^o(k) & D_{21}^o(k) \end{bmatrix} = \begin{bmatrix} C_2^o(k+N) & D_{21}^o(k+N) \end{bmatrix}$. Here, N represents the number of servo sectors.

III. Optimal H_∞ Control for HDD Servo Systems with an Irregular Sampling Rate

A. Optimal H_∞ control formulation

In order to deal with the HDD plant variations and missing PES samples, we will extend well-known H_∞ LTI error rejection loop shaping design techniques for HDDs with regular sampling rates to irregular sampling rates. To do so, the H_∞ norm of linear time-invariant systems must be generalized as ℓ_2 induced norm for LPTV systems. For an LPTV system H with input w and output z, its ℓ_2 induced norm is defined as

$$\|H\|_{2\leftarrow 2} = \left(\sup_{w \in \ell_2 \setminus \{0\}} \frac{\sum_{k=0}^{\infty} z^T(k) z(k)}{\sum_{k=0}^{\infty} w^T(k) w(k)} \right)^{1/2} \,. \tag{3}$$

For the H_∞ control of LPTV systems, we need to design

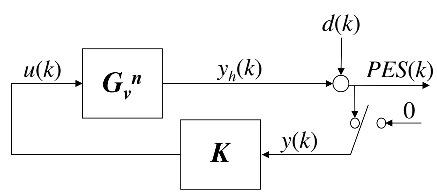

Fig. 2. The HDD servo system with the nominal VCM plant

a controller K satisfying the following conditions for the nominal VCM plant G_v^n:

$$\left\| \begin{bmatrix} T_s \cdot W_p & T_c \cdot W_\triangle \end{bmatrix} \right\|_{2\leftarrow 2} < 1 \tag{4}$$

where T_s is the sensitivity function (i.e. error rejection transfer function) from d to PES, as shown in Fig. 2, while T_c is the complementary sensitivity function from d to the plant output y_h. The W_p and $W_\triangle$ in (4) are the loop-shaping performance weighting function and the plant uncertainty weighting function respectively. It is known that Equation (4) guarantees the robust performance that the magnitude of the obtained error rejection function (for single-input-single-output (SISO) systems) is always smaller than $\left|W_p(e^{j\omega})\right|^{-1}$ for the uncertain plant characterized in (1).

Similar to the optimal H_∞ control of HDD servo systems with multi-rate sampling and actuation in [9], we consider the block diagram shown in Fig. 3 for the control design of the servo systems with an irregular sampling rate. In the figure, W_u is the control input weighting value to be tuned so that the inequalities in (4) hold. As discussed in [9], this control design formulation is different from the standard H_∞ control problem formulation [13] due to the introduction of the fictitious disturbance w_2 and the fact that the performance

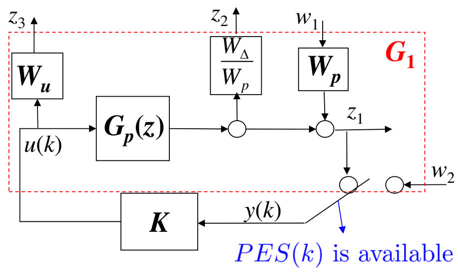

Fig. 3. Control design formulation

weighting function was moved to the disturbance input side. As a result, the constraint $D_{21}(k)D_{21}^T(k) \succ 0$ for all k in the developed control synthesis in [9] is satisfied. As will be shown subsequently, the introduction of w_2 does not affect the optimal H_∞ controller and the optimal closed-loop ℓ_2 induced norm at all. Moreover, by changing the position of the performance weighting function, the feedback signal y is affected by the "colored" disturbance ($W_p w_1$) more directly when missing samples occur.

With these changes and utilizing the block diagram in Fig. 3, the optimal H_∞ control problem is to find an optimal linear time-varying controller K and a minimum γ with the closed loop ℓ_2 induced norm less than γ, i.e.

$$\begin{array}{ll} \min_{K,\gamma} & \gamma \\ \text{s.t.} & \|T_{z\leftarrow w}\|_{2\leftarrow 2} < \gamma \end{array} \tag{5}$$

where $T_{z\leftarrow w}$ represents the transfer function matrix from $w = \begin{bmatrix} w_1 & w_2 \end{bmatrix}^T$ to $z = \begin{bmatrix} z_1 & z_2 & z_3 \end{bmatrix}^T$. Suppose that the LPTV system G_1 (with input $\begin{bmatrix} w_1 & w_2 & u \end{bmatrix}^T$ and output $\begin{bmatrix} z_1 & z_2 & z_3 & y \end{bmatrix}^T$) shown in Fig. 3 can be represented by the following state-space realization:

$$G_1 \sim \begin{bmatrix} x(k+1) \\ z(k) \\ y(k) \end{bmatrix} = \left[\begin{array}{c|cc} A & B_1 & B_2 \\ \hline C_1 & D_{11} & D_{12} \\ C_2(k) & D_{21}(k) & 0 \end{array}\right] \begin{bmatrix} x(k) \\ w(k) \\ u(k) \end{bmatrix} \tag{6}$$

with

$$\begin{bmatrix} C_2(k) & D_{21}(k) \end{bmatrix} = \begin{cases} \begin{bmatrix} C_{2m} & \begin{bmatrix} D_{21m} & 0 \end{bmatrix} \end{bmatrix} & \text{if } PES(k) \text{ is available} \\ \begin{bmatrix} 0 & \begin{bmatrix} 0 & 1 \end{bmatrix} \end{bmatrix} & \text{otherwise} \end{cases}$$

In (6), all of matrix entries except $C_2(k)$ and $D_{21}(k)$ are constant and $C_2(k)$ and $D_{21}(k)$ are periodic with period N.

For the control synthesis in the next section, we will use the following notation, $B = \begin{bmatrix} B_1 & B_2 \end{bmatrix}$, $D_{1\bullet} = \begin{bmatrix} D_{11} & D_{12} \end{bmatrix}$, $C(k) = \begin{bmatrix} C_1 \\ C_2(k) \end{bmatrix}$, and $D_{\bullet 1}(k) = \begin{bmatrix} D_{11} \\ D_{21}(k) \end{bmatrix}$.

B. Optimal H_∞ control synthesis

As mentioned in [9], there may exist many controllers that satisfy the inequality in (5) for a given γ. Similar to [9], we would like to obtain the minimum entropy controller [11] among all these controllers. In order to synthesize the optimal H_∞ controller, we first need to obtain the unique minimum entropy controller satisfying the ℓ_2 induced norm constraint in (5) with a fixed γ, and then utilize a bi-section search method to find the minimum γ and the corresponding optimal controller. In the minimum entropy control synthesis methodology that follows, for simplicity and without loss of generality, we will assume that $\gamma = 1$.

Utilizing the control design methodology presented in [9], we obtain the following unique stabilizing minimum entropy time-varying controller K, which satisfies the constraint in (5) and is given by the following state space realization:

$$\begin{cases} \hat{x}(k+1) = \bar{A}\hat{x}(k) + B_2 u(k) + F_t(k)\left(\bar{C}_2(k)\hat{x}(k) - y(k)\right) \\ u(k) = -T_{22}^{-1}\bar{C}_{12}\hat{x}(k) + L_t(k)\left(\bar{C}_2(k)\hat{x}(k) - y(k)\right) \end{cases} \tag{7}$$

Notice that for the irregular sampling rate HDD servo system shown in (6), all matrix entries in the state-space realization (6) are constant except $C_2(k)$ and $D_{21}(k)$. Consequentially, the controller synthesis algorithm utilized to calculate the control parameters in (7) can be furthermore simplified as follows.

1) Solve the state-feedback algebraic Riccati equation:

$$X = A^T X A + C_1^T C_1 - M\left(R + B^T X B\right)^{-1} M^T$$

where $M = A^T X B + C_1^T D_{1\bullet}$.

2) Define $T = \begin{bmatrix} T_{11} & 0 \\ T_{21} & T_{22} \end{bmatrix}$ with $T_{11} \succ 0$ and $T_{22} \succ 0$, and compute T using:

$$R + B^T X B = T^T J T$$

where $R = D_{1\bullet}^T D_{1\bullet} - \begin{bmatrix} I & 0 \\ 0 & 0 \end{bmatrix}$, $J = \begin{bmatrix} -I & 0 \\ 0 & I \end{bmatrix}$.

3) Get $\begin{bmatrix} F_1 \\ F_2 \end{bmatrix} = \left(R + B^T X B\right)^{-1} M^T$.

4) Calculate the following matrices for the filtering Riccati equation: $\bar{A} = A + B_1 F_1$, $\bar{C}_2(k) = C_2(k) + D_{21}(k) F_1$, and $\bar{C}_{12} = -T_{22} F_2$. Let $D_\perp$ be an orthogonal matrix to D_{12}. In addition, define a matrix W such that $W^T W = I - T_{11}^T T_{11}$ and W has appropriate dimensions so that the following matrix multiplication is well defined:

$$\begin{bmatrix} \bar{D}_{111} \\ \bar{D}_{112} \end{bmatrix} = D_\perp W + D_{12} T_{21} \, .$$

5) Update forwards in time the filtering Riccati equation solution with zero initial condition:

$$Y(k) = \bar{A} Y(k-1) \bar{A}^T + B_1 B_1^T - \tilde{M}(k) \left(\tilde{R}(k) + \begin{bmatrix} \bar{C}_{12} \\ \bar{C}_2(k) \end{bmatrix} Y(k-1) \begin{bmatrix} \bar{C}_{12} \\ \bar{C}_2(k) \end{bmatrix}^T \right)^{-1} \tilde{M}^T(k)$$

where $Y(k) \succeq 0$ and

$$\tilde{M}(k) = \bar{A} Y(k-1) \begin{bmatrix} \bar{C}_{12} \\ \bar{C}_2(k) \end{bmatrix}^T + B_1 \begin{bmatrix} \bar{D}_{112} \\ D_{21}(k) \end{bmatrix}^T .$$

6) Define $\tilde{T}(k) = \begin{bmatrix} \tilde{T}_{11}(k) & \tilde{T}_{12}(k) \\ 0 & \tilde{T}_{22}(k) \end{bmatrix}$, with $\tilde{T}_{11} \succ 0$ and $\tilde{T}_{22} \succ 0$, and compute $\tilde{T}(k)$ using

$$\tilde{R}(k) + \begin{bmatrix} \bar{C}_{12} \\ \bar{C}_2(k) \end{bmatrix} Y(k-1) \begin{bmatrix} \bar{C}_{12} \\ \bar{C}_2(k) \end{bmatrix}^T = \tilde{T}(k) \tilde{J} \tilde{T}^T(k)$$

where

$$\tilde{R}(k)=\begin{bmatrix}\bar{D}_{112}\\ D_{21}(k)\end{bmatrix}\begin{bmatrix}\bar{D}_{112}\\ D_{21}(k)\end{bmatrix}^T-\begin{bmatrix}I & 0\\ 0 & 0\end{bmatrix}, \tilde{J}=\begin{bmatrix}-I & 0\\ 0 & I\end{bmatrix}.$$

7) Obtain

$$\begin{bmatrix}\tilde{F}_1(k)\\ \tilde{F}_2(k)\end{bmatrix}=\left(\tilde{R}(k)+\begin{bmatrix}\bar{C}_{12}\\ \bar{C}_2(k)\end{bmatrix}Y(k-1)\begin{bmatrix}\bar{C}_{12}\\ \bar{C}_2(k)\end{bmatrix}^T\right)^{-1}\times \tilde{M}^T(k)$$

8) Calculate the filter gains $L_t(k)=T_{22}^{-1}(k)\tilde{T}_{12}(k)\tilde{T}_{22}^{-1}(k)$ and $F_t(k)=\tilde{F}_1^T(k)\tilde{T}_{12}(k)\tilde{T}_{22}^{-1}(k)+\tilde{F}^T(k)$.

Since, as proved in [9], the Riccati equation solution $Y(k)$ in step 5) is periodic, $Y(k)$ computed "forwards" in time with zero initial condition converges to a steady-state periodic solution with period N. It turns out that the filter gains $F_t(k)$ and $L_t(k)$ are also periodic with period N. In addition, it is straightforward to show that both $\tilde{T}_{12}(k)$ and $\tilde{F}_{12}(k)$ are equal to 0 at the instance k when PES is unavailable. Thus, both $F_t(k)$ and $L_t(k)$ are also equal to 0 at the time when $PES(k)$ is unavailable, which verifies the claim that the fictitious disturbance w_2 does not affect the optimal H_∞ controller. With the zero gains of $F_t(k)$ and $L_t(k)$ at the instance when a missing PES sample occurs, the time varying control parameter $\bar{C}_2(k)=C_2(k)+D_{21}(k)F_1$ in (7) can be simply substituted by a constant parameter $\bar{C}_{2m}=C_{2m}+\begin{bmatrix}D_{21m} & 0\end{bmatrix}F_1$ without changing the controller effect. As a result, for the HDD servo systems with missing PES samples, all of the control parameters of the minimum entropy H_∞ controller shown in (7) except $F_t(k)$ and $L_t(k)$ are constant.

IV. Control Synthesis Application to a Real HDD

In order to evaluate our proposed optimal H_∞ control methodology in this paper, the algorithm will be applied to the track-following control of a real hard disk drive with missing PES samples through both simulation and implementation studies. The hard disk drive considered here was provided by Western Digital Corporation. For this 3.5" desktop disk drive, the number of servo sectors is $N=256$ and the spindle rotation speed is 7200 RPM. In addition, the servo patterns on some servo sectors at the inside diameter (ID) have been damaged and thus PES on these servo sectors is unaccessible to the servo system. Specifically, we found that PES is unaccessible on the following 51 servo sectors: $M_{\text{miss}}=\{i:$ PES is unaccessible on servo sector $i\}=\{0,$ 4, 8, 17, 21, 25, 34, 38, 42, 47, 51, 55, 59, 64, 68, 72, 81, 85, 89, 98, 102, 106, 111, 115, 119, 123, 128, 132, 136, 145, 149, 153, 162, 166, 170, 179, 183, 187, 192, 196, 200, 209, 213, 217, 226, 230, 234, 239, 243, 247, 251$\}$.

A. Modeling of the real HDD

In order to obtain the model of the voice coil motor plant, the actual VCM plant (including notch filters [12]) frequency response for the considered disk drive was measured on the disk area where there are no damaged servo sectors. Then, the nominal VCM model $G_v^n(s)$ was identified to match the experiment frequency response, as described in [10]. Note that in order to reduce the control order, the nominal VCM plant was just identified as an 8th order model.

The open-loop PES nonrepeatable runout (NRRO) power spectrum was reconstructed by measuring the closed-loop NRRO power spectrum and the error rejection function and then dividing the closed-loop NRRO power spectrum by the measured error rejection function. The inverse of the resulting open-loop NRRO power spectrum density is shown in Fig. 4. In order to attenuate disturbances, the performance weighting function W_p was approximately chosen as the scaled open-loop NRRO power spectrum density. The inverse of the frequency response for the designed performance weighting function is also shown in Fig. 4.

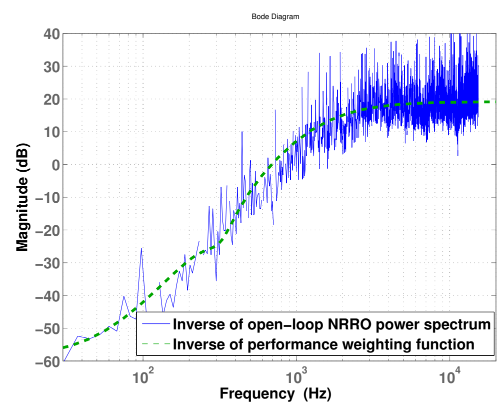

Fig. 4. The performance weighting function inverse and the inverse of the open-loop PES NRRO power spectrum

The uncertainty weighting function considered in the control design is shown in Fig. 5. The chosen uncertainty weighting function demonstrates that the plant could have an unstructured uncertainty producing a $\pm 28\%$ gain variation at low frequency and a $\pm 175\%$ gain variation at high frequency.

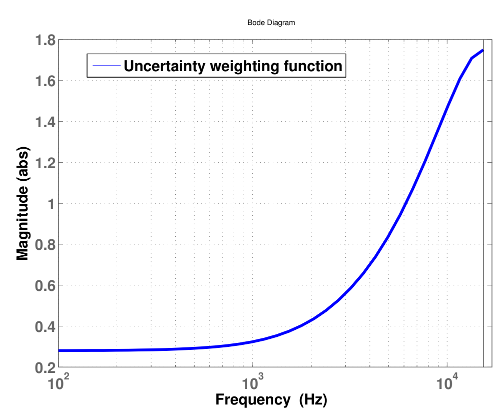

Fig. 5. Plant uncertainty weighting function $W_\triangle$

B. Control design and simplification

It is well know that if the optimal H_∞ controller yields a minimum $\gamma^* \leq 1$, then the controller is able to achieve the robust performance with the performance weighting function shown in (4). In other words, the designed controller achieves the better disturbance attenuation than the inverse of performance weighting function shown in Fig. 4 for all the plant variations with the multiplicative plant uncertainty weighting function in Fig. 5. With the determined performance weighting function and plant uncertainty function, the weighting value W_u is to be tuned so that the achieved γ is less than or equal to 1 and simultaneously the control actuation generated by the resulting control K is appropriate under the hardware constraints of real HDD servo systems.

For the real hard disk drive described in the previous section, a weighting value of $W_u = 4$ was selected and thus the resulting optimal H_∞ control is able to achieve an optimal ℓ_2 induced norm $\gamma^* = 0.91$. Moreover, the resulting gains $F_t(k)$ and $L_t(k)$ in (7) are zero when the measurement signal PES is unavailable at the instance k. The designed gain $L_t(k)$ for one revolution is shown in Fig. 6.

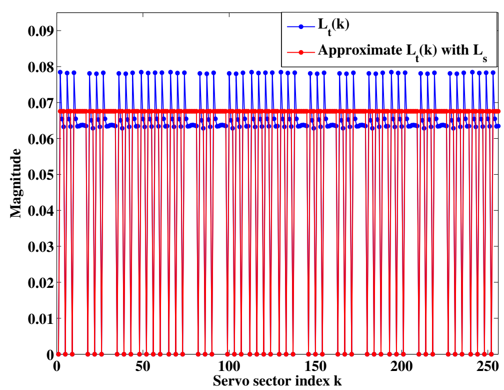

Fig. 6. The designed $L_t(k)$

Since the control parameters $F_t(k)$ and $L_t(k)$ are time-varying, we have to save all 205 ($= 256 - 51$) sets of non-zero time-varying control parameters, requiring a significant amount of memory. Unfortunately, it is almost impossible to reserve so much memory for storing the control parameters in real HDDs. Fortunately, we found that the non-zero time-varying parameters $F_t(k)$ and $L_t(k)$ have very small variations, which motivates us to treat all non-zero time-varying control parameter values as constants. Specifically, the constant values F_s and L_s for $F_t(k)$ and $L_t(k)$ are obtained by taking the average of all non-zero $F_t(k)$ and $L_t(k)$ respectively. Then, the approximate control parameters F_s and L_s will be applied when PES is available. Consequentially, just one set of control parameters F_s and L_s has to be stored in memory. The approximate values with L_s for $L_t(k)$ are also shown in Fig. 6. The simulation study, which will be presented in next section, shows that such control parameter approximation has a tolerable negative affect on the control performance.

TABLE I
SIMULATION RESULTS

	3σ PES (% track)	
	Nominal	Worst
With the original control parameters $F_t(k)$ and $L_t(k)$	2.83	3.66
With the approximate control parameters using F_s and L_s	2.84	3.70

C. Simulation study

In order to evaluate the robust performance of the designed controller, a total of 50 different VCM plants was collected. These various VCM plants were randomly generated based on the identified nominal VCM plant and the uncertainty weighting function shown in Fig. 5 by using Matlab function "`usample`".

The simulation results of the Root Mean Square (RMS) 3σ values of PES for the nominal plant and the worst-case plant are illustrated in Table I. Based on these time-domain simulation results, we are confident that the proposed optimal H_∞ control indeed attains its predicted the robust performance. Moreover, the simulation results demonstrate that the performance degradation caused by the control parameter approximation is so small that the control simplification presented in the previous section is viable.

D. Control Implementation study

The simulation results presented in the previous subsection illustrate that the proposed control design methodology in this paper is able to handle an irregular sampling rate and achieve robust performance. In this subsection, we discuss its implementation on an actual HDD with missing PES samples. The designed controller was coded on the disk drive's own processor by changing its firmware code. Then, the designed optimal H_∞ control was tested and evaluated in the disk area where the missing PES samples happen with the sampling missing sequence of M_{miss} as illustrated in the previous section.

Unlike linear time-invariant systems, the linear time-varying system with the irregular sampling rate has no well-defined error rejection transfer function. However, in order to evaluate the implemented controller for the considered disk drive, we define the following disturbance-PES relationship called approximate error rejection function. A sweep sinusoid excitation is injected into the position of the disturbance d shown in Fig. 1, which is the same as the way that the excitation is injected for measuring the error rejection function for disk drives with a regular sampling rate. Then, the PES response caused by the excitation is collected. Since PES is unaccessible at the time when missing samples happen, we approximately treat the previous available PES as the current unavailable PES. Afterwards, the discrete Fourier transform (DFT) is computed for the collected PES data and then the DFT component at the frequency of the sinusoid excitation is identified. Consequentially, the approximate frequency response from the disturbance d to PES is calculated by dividing the identified PES DFT component by the corresponding excitation DFT component. As shown by the blue line in Fig. 7, the approximate error rejection function was measured during the experimental study.

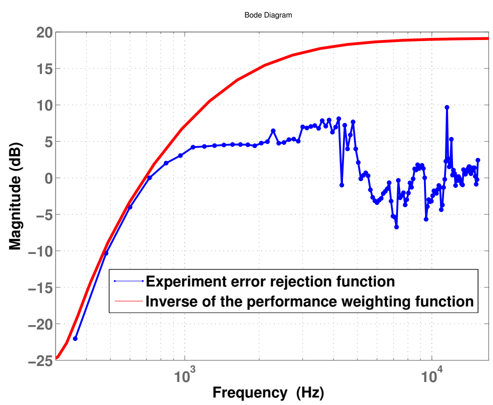

Fig. 7. Experiment result for error rejection function

The inverse of the performance weighting function is also shown in Fig. 7. Since the achieved optimal ℓ_2 induced norm is less than 1, the measured approximate error rejection function should be below the inverse of the performance weighting function at every frequency, which is verified by the experiment results shown in Fig. 7. Thus, the experiment results demonstrate that the optimal H_∞ control synthesized by our proposed control algorithm achieves the desired disturbance attenuation. In addition, 3σ value for the closed-loop NRRO PES with the implemented control is 2.36% of track width. However, note that such experiment result is a little bit different from the simulation 3σ PES shown in Table I. The reason may be because the fitted VCM model is not exactly the same as the real disk drive and the identified open-loop disturbance in simulation is different from the real disturbance especially at low frequency where the disturbance is quite difficult to be modeled.

V. CONCLUSION

Irregular sampling rates are sometimes unavoidable in hard disk drive servo systems, for example, when false PES demodulation is caused by damaged servo sectors or when the unavailability of the feedback PES is due to so called collisions in the self-servo track writing process. By considering that the position of the unavailable feedback signal is fixed and the natural periodicity of HDDs is related to the disk rotation, the servo systems with irregular sampling rates were modeled as linear periodically time-varying systems. In addition, since there tend to be large variations in HDD dynamics due to variations in manufacturing and assembly, the designed controllers must guarantee a pre-specified level of performance for a large set of HDDs. By using classical loop-shaping ideas, the H_∞ loop-shaping control can be conveniently designed to deal with the robust performance of the designed loop shape. Based on the optimal H_∞ control synthesis algorithm [9] for general LPTV systems, the optimal H_∞ control algorithm was developed for HDD servos with irregular sampling rates in this paper. Consequentially, the proposed control synthesis technique is able to conveniently design loop-shaping control and to achieve the robust performance of a desired error rejection function for disturbance attenuation in the case of irregular sampling rates. The proposed controller was applied to an actual HDD which had an irregular sampling rate due to damaged servo sectors. Results obtained from both simulation and experimental studies demonstrated the synthesized controller's effectiveness in handling an irregular sampling rate and achieving the robust performance. Moreover, simulation results were validated by the obtained experiment results.

VI. ACKNOWLEDGMENTS

The two UC Berkeley authors would like to thank Western Digital Corporation for providing invaluable information to perform this study. This work was performed with the support of the UC Berkeley Computer Mechanics Laboratory (CML) and a research grant from Western Digital Corporation.

REFERENCES

[1] D. Abramovitch, T. Hurst, and D. Henze, 1998. "An overview of the PES Pareto method for decomposing baseline noise sources in hard disk position error signals," *IEEE Trans. On Magnetics*, vol. 34, no. 1, pp. 17-23.

[2] D. Brunnett, Y. Sun, and L. Guo, 2007. "Method and apparatus for performing a self-servo write operation in a disk drive using spiral servo information," U.S. Patent 7230789B1.

[3] B. Chen, T. Lee, and V. Venkataramanan. *Hard Disk Drive Servo Systems*, Adavances in Industrial Control Series, Springer, New Your, 2006.

[4] R. Conway, 2007. "Multi-objective Control Design for Discrete Time Periodic Systems via Convex Optimization", Master report, University of California, Berkeley.

[5] R. Conway and R. Horowitz, 2009. "Analysis of H_2 Guaranteed Cost Performance," *Proceedings of the 2009 Dynamic Systems and Control Conference*, Hollywood, California.

[6] R. Ehrlich, 2005. "Methods for Improving Servo-Demodulation Robustness," U.S. Patent 6943981B2.

[7] M. Hirata, K. Liu, T. Mita, and T. Yamaquchi, 1992. "Head positioning of a hard disk drive using H theory," *Proceedings of the 31st IEEE Conference on Control and Decision*, vol. 1, pp. 2460-2461.

[8] R. Nagamune, X. Huang, and R. Horowitz, 2005. "Multi-rate track-following control with robust stability for a dual-stage multi-sensing servo systems in HDDs," *Proceedings of the Joint 44th IEEE Conference on Decision and Control and European Control Conference*, pp.3886-3891.

[9] J. Nie, R. Conway, and R. Horowitz. "Optimal H_∞ Control for Linear Periodically Time-Varying Systems in Hard Disk Drives", submitted to *the 3rd Dynamic Systems and Control Conference*.

[10] J. Nie and R. Horowitz, "Design and Implementation of Dual-Stage Track-Following Control for Hard Disk Drives", *Proceedings of the Dynamic Systems and Control Conference*, Hollywood, California

[11] M. A. Peters and P. A. Iglesias. *Minimum Entropy Control for Time-Varying Systems*. Birkhäuser, Boston 1997.

[12] T. Semba, N. Kagami and A. Tokizono, 2001. "Method and apparatus for suppressing mechanical reasonance in a disk drive storage device using a notch filter", US Patent 6219196.

[13] S. Skogestad and I. Postlethwaite. *Multivariable feedback control: analysis and design*, John Wiley, Hoboken, NJ 2005.